

# Analysis of the tropical climate variability in a two-column framework

Gilles Bellon · Guillaume Gastineau ·  
Aurélien Ribes · Hervé Le Treut

Received: 16 November 2009 / Accepted: 1 June 2010 / Published online: 17 June 2010  
© Springer-Verlag 2010

**Abstract** This work examines the relevance of a classical two-column modeling framework of the tropical climate in terms of observed natural variability. A method is developed to analyze the observed tropical climate in a simple framework that features a moist, ascending column and a dry, subsiding one. This method is used to analyze the natural variability of the tropical climate in the ERA40 reanalysis and in ISCCP satellite data. It appears that the seasonal cycle of the tropic-wide sea surface temperature (SST) is almost linearly linked to the seasonal cycle of the relative area of the moist regions, as predicted by the sensitivity of the two-column models. A more detailed analysis shows that this link is the product of a complex interaction and adjustments between the moist and dry regions. The seasonal cycle of low-cloud cover in the dry regions also appears to interact with the SST seasonal cycle: the low-cloud cover influences the tropic-wide SST via its direct radiative forcing on the local SST and it appears to be controlled by the SST difference between moist and dry regions. By contrast, the SST interannual variability appears to be driven by the El Niño Southern Oscillation (ENSO), with no significant impact from the changes in the relative area of the moist regions or in the

low-cloud cover in the dry regions independently of the ENSO. ENSO-related changes in the area of moist regions and low-cloud cover constitute negative feedbacks on the ENSO-related SST variability.

**Keywords** Tropical climate · Idealized framework

## 1 Introduction

The tropical free troposphere is characterized by the homogeneity of the temperature profiles, which is necessary to ensure consistency with the large-scale circulation (Held and Hou 1980), and by the bimodality of the humidity profiles (Zhang et al. 2003). On large scales, this bimodality manifests itself as alternating moist, precipitating regions, which constitute the tropical convergence zones (TCZs), and arid areas. This alternation is embedded in the large-scale Hadley and Walker circulation: the dry air subsides, whereas the moist, convective columns exhibit mean upward motion. Single-column models (SCMs) exhibit multiple equilibria that correspond to atmospheric columns in one of these two states. Radiative-convective SCMs (Rennó 1994; Ide et al. 2001), as well as SCMs with a parameterization of large-scale dynamics (Sobel et al. 2007), exhibit one dry, shallow-convective equilibrium along with a moist, precipitating one. Large-scale dynamics are crucial to the stability of the convective columns, which can otherwise be in a state of runaway greenhouse: the energy emitted to space decreases with increasing SST, leading to a constant warming of the column. These observed features and model results have inspired a two-column conceptual approach in the study of the tropical atmosphere. It has been shown that spontaneous large-scale circulations can arise from radiative-convective feedbacks

---

G. Bellon (✉)  
Centre National de Recherches Météorologiques,  
CNRS and Météo France, 42, avenue Gaspard Coriolis,  
31057 Toulouse Cedex 01, France  
e-mail: gilles.bellon@meteo.fr

G. Gastineau · H. Le Treut  
Laboratoire de Météorologie Dynamique, Institut Pierre-Simon  
Laplace, CNRS and Ecole Normale Supérieure, Paris, France

A. Ribes  
Centre National de Recherches Météorologiques,  
CNRS and Météo France, Toulouse, France

(Raymond and Zeng 2000), and that sufficiently strong circulations cause the bimodality of the humidity profiles (Nilsson and Emanuel 1999).

Pierrehumbert (1995) was the first to propose a simple two-column climate model, as illustrated in Fig. 1, aimed at representing the basic interaction between radiation and dynamics in the tropical climate. His work showed that the stability of the observed tropical climate relies on the coupling of the dry and moist regions by the large-scale circulation. This circulation creates a stable climate by exporting the excess energy from the convective, runaway-greenhouse column to the subsiding one, where it is radiated away to space (Pierrehumbert 1995). This type of model solves the water and energy budgets of one or two atmospheric boxes in each column, with idealized vertical profiles of temperature and humidity. As a result, the overturning circulation between the columns is controlled by the heat budget of the subsiding free troposphere. There, at equilibrium, the radiative cooling must be compensated by the vertical advection of static energy. The vertical speed is therefore constrained by the radiative cooling, and the intensity of the large-scale circulation is proportional to this radiatively-constrained vertical speed and the size of the subsiding column (Larson et al. 1999; Bellon et al. 2003).

This family of models provides an alternative to the common approach, which studies climate feedbacks in one atmospheric column or in a collection of atmospheric columns (e.g., Bony et al. 1997; Bony and Dufresne 2005). It allows one to consider the zeroth-order interaction between the radiative-convective feedbacks in moist regions of the tropics and those in dry regions. This interaction is associated with the large-scale circulation. These two-column models were therefore used extensively to study the feedbacks that regulate the sensitivity of the tropical climate (Miller 1997; Larson et al. 1999; Bellon et al. 2003). In particular, with these models, the weak variability of the tropical Sea Surface Temperature (SST) on decadal to millennial time scales can be explained by a

negative feedback involving the response of the large-scale tropical circulation to climate perturbations. However, these models show a large sensitivity to some of their fixed parameters that vary in the real world and could therefore allow additional feedbacks. One of these parameters is the relative sizes of the dry and moist columns (Pierrehumbert 1995; Larson et al. 1999; Bellon et al. 2003). When the size of the moist column increases, the average greenhouse effect increases as well. The decrease in the size of the dry column also decreases the intensity of the large-scale circulation. The associated large-scale redistribution of energy is thus reduced and this enhances the warming. The resulting strong sensitivity of the SST to the size of the columns is a robust feature of this family of models.

Another study (Miller 1997) focused on the potential feedbacks involving stratocumulus clouds in the subsiding regions of the tropics. In the case of a doubling of the atmospheric concentration of carbon dioxide, Miller (1997)'s model shows an increase of low-cloud cover in the subsiding column resulting from an increase in lower-tropospheric stability (Klein and Hartmann 1993). Because the albedo effect of these clouds is far more important than their additional infra-red contribution, this constitutes a negative feedback on the greenhouse warming. Low-cloud feedbacks have been shown to be responsible for most of the spread in the response of general circulation models (GCMs) to anthropogenic climate change (Bony and Dufresne 2005; Dufresne and Bony 2008). Some GCM studies have suggested that the low-cloud feedback to climate change is negative (Zhu et al. 2007) but a recent study that evaluates the skill of GCMs to reproduce the observed relationships between cloudiness and large-scale variables shows that the one GCM that simulates correctly all these relationships predicts a positive low-cloud feedback to anthropogenic climate change (Clement et al. 2009).

If the relative area of the moist regions and the low-cloud cover in the dry regions contribute to the natural variability in the present climate, we can expect the feedbacks resulting from their variations to be relevant in the context of climate change. The present work is a first step in understanding whether such feedbacks between the SST and the relative area of the moist regions or the low-cloud cover in the subsiding regions exist in the real world. Whereas extensive modeling studies have been undertaken in this two-column framework, little has been done to show how the observed tropical atmosphere can be interpreted and analyzed following this conceptual framework. The purpose of this paper is to propose a method for analyzing global datasets in the two-column framework presented above (Sect. 2), and to show how the natural variability of the tropical climate relates to natural variations of the observed equivalents of simple-model parameters (Sect. 3).

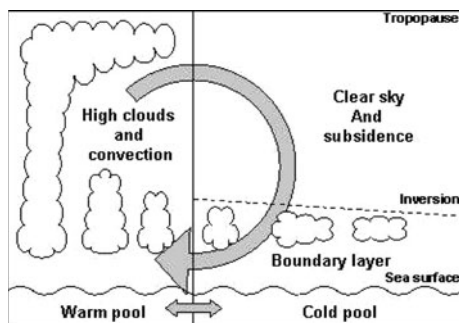


Fig. 1 Schematic two-column model diagram

## 2 Applying a two-column framework to global datasets

### 2.1 Datasets

We use 392 months of the European Centre Medium-Range Weather Forecast 40-year Reanalysis (ERA40, Simmons and Gibson 2000), from January 1970, to August 2002, to determine the extent of the tropical belt and distinguish between moist and dry regions. We use the monthly mean fields with a  $1.125^\circ \times 1.125^\circ$  resolution on the horizontal. Using this dataset for the satellite period only (1979 onwards) yields results similar to those presented here. The reanalyzed cloud fields are essentially produced by the GCM used by ERA40, and they have been shown to exhibit significant biases when compared to campaign observations (Cronin et al. 2006; Stevens et al. 2007). Considering these limitations of reanalyzed cloud fields, we also use satellite data from the International Satellite Cloud Climatology Project (ISCCP, Schiffer and Rossow 1983). We use the monthly fields of low-cloud covers from July, 1983, to August, 2002 (230 months). ISCCP data comes on a 280-km, equal-area grid. We interpolate this dataset on the ERA40 grid by dividing each ERA40 gridbox in tiles belonging to different ISCCP gridboxes and taking the area-weighted average of these tiles' ISCCP cloudiness to be the ERA40 gridpoint cloudiness.

### 2.2 Defining the tropical belt

We define the tropics as the region where the monthly-mean, zonal-mean Hadley circulation is enclosed. A classical way to describe the Hadley circulation is the Stokes streamfunction  $\Psi$  that measures the total northward (respectively southward) transport of mass below (respectively above) the level considered across the latitude considered (Oort and Rasmusson 1970):

$$\Psi = \frac{2\pi R \cos \phi}{g} \int_p^{p_s} \bar{v} dp' = -\frac{2\pi R^2}{g} \int_{\phi_{SP}}^{\phi} \bar{\omega} \cos \phi' d\phi', \quad (1)$$

where  $p$  is the pressure and  $\phi$  the latitude,  $p_s$  the surface pressure and  $\phi_{SP}$  the latitude of the South Pole.  $v$  and  $\omega$  are the meridional and the vertical speed in pressure coordinates,  $R$  is the Earth radius, and the overbar stands for zonal averaging. The zonal-mean circulation is closed between two zero isolines of  $\Psi$ . One of  $\Psi$ 's zero isolines is close to a vertical line within ten degrees of latitude from the Equator, and the boreal (respectively austral) Hadley cell extends between this zero isoline and the following one in the Northern (respectively Southern) Hemisphere. Here, the tropics are defined as the area encompassing the two

Hadley cells, and the boundaries of the tropical belt are defined as the poleward boundaries of the gridpoints where  $\Psi$  changes sign at 500 mb. The total area of the tropics  $A_t$  is computed between these two latitudinal boundaries. The tropic-wide or tropical SST is the average SST over the oceans within this belt.

### 2.3 Defining a humidity threshold

To distinguish between the dry and moist regions of the tropics, we use the column relative humidity (CRH), computed from the ERA40 humidity and temperature fields. The CRH is the ratio of the column-integrated water vapor to the column-integrated saturation water vapor:

$$CRH = \frac{\int_{p_t}^{p_s} q dp}{\int_{p_t}^{p_s} q^*(T, p) dp}, \quad (2)$$

where  $p_t$  is the pressure at the tropopause,  $q$  is the specific humidity, and  $q^*(T, p)$  is the saturation specific humidity at the temperature  $T$  and pressure  $p$ .

Bretherton et al. (2004) showed that precipitation over the tropical oceans is tightly related to CRH. This humidity variable filters out the influence of the temperature on the column integrated water vapor and therefore appears to be a good candidate for discriminating between moist, precipitating columns and non-precipitating, dry ones. Figure 6 in Bretherton et al. (2004) shows that precipitation in 75% of the atmospheric columns with  $CRH = 50\%$  is negligible (inferior to 1 mm/day), while 75% of the atmospheric columns with  $CRH = 60\%$  exhibit significant precipitation (more than 1 mm/day). Therefore, a threshold between 50% and 60% appears suitable to distinguish between dry and precipitating regions. The results in the next section are shown for a threshold  $CRH_t = 55\%$ , and sensitivity studies showed that our results are not very sensitive to the precise choice of threshold.

The total area  $A_m$  of the moist regions is defined as the area with  $CRH > CRH_t$  and the relative area  $A$  of the moist regions is defined by the ratio of  $A_m$  to  $A_t$ :  $A = A_m/A_t$ . The low-cloud cover  $LCC$  (respectively  $LCC_r$ ) in the dry regions is the average ISCCP (respectively ERA40) low-cloud amount over the regions with  $CRH < CRH_t$ . The intensity of the overturning circulation  $\Phi$  is computed by integrating the vertical speed  $\omega$  at 500 mb over the dry regions (by our definition of the tropical belt, this is equivalent to integrating  $-\omega$  at 500 mb over the moist regions, we found an error of less than 1% between the two measures), normalized by the size of the tropics  $A_t$ .

### 3 Natural variability of the tropical climate in the two-column framework

#### 3.1 Seasonal cycle

The climatological seasonal cycle of the SST, relative area  $A$  of the moist regions, reanalyzed low-cloud cover  $LCC_r$ , and intensity of the overturning circulation  $\Phi$  are computed using all 392 months of the ERA40 reanalysis. That of the ISCCP low-cloud cover in the dry regions  $LCC$  is computed using the 230 months of the ISCCP series. The seasonal cycles of SST,  $A$ ,  $LCC_r$ , and  $\Phi$  computed over the same 230 months are almost identical to the ones we display, so the use of different time series does not seem to affect our results.

Figure 2 shows the seasonal cycles of tropical SST, moist-region SST ( $SST_m$ ) and dry-region SST ( $SST_d$ ) and their difference  $\Delta SST$ , as well as the seasonal cycles of  $LCC$ ,  $LCC_r$ ,  $A$  and  $\Phi$ . The reanalyzed low-cloud cover  $LCC_r$  is about 25% smaller than the ISCCP  $LCC$ , a bias that has been identified in previous work (Jakob 1999). Its seasonal cycle is also significantly different from the seasonal cycle of  $LCC$ , with a minimum during boreal spring versus an extended  $LCC$  minimum during boreal winter. In general, systematic biases have been found in reanalyzed cloud fields (Weare 2000) and we will focus here on the ISCCP  $LCC$ .

The tropical SST has a maximum during the boreal spring associated with a maximum of  $A$  (Fig. 2a,d). The seasonal cycle of tropical SST is highly correlated to that of  $A$  (0.91, maximum at zero lag); it suggests a strong interaction between SST and  $A$  at seasonal timescales: warm SST favors convection, which increases  $A$ , and variations in  $A$  change the radiative budget and the large-scale circulation of the tropical climate system. The respective magnitudes of the seasonal cycles of SST and  $A$  are consistent with the sensitivity of simple two-column models (Bellon et al. 2003), suggesting that changes in  $A$  can account for a significant fraction of the SST variations. The seasonal cycle of  $\Phi$  appears to be, to some extent, in phase opposition with the seasonal cycle of  $A$  (Fig. 2e). This is expected since  $\Phi \propto (1 - A) * w$ , where  $w$  is the average subsidence in the dry regions. It tends to support the existence of a dynamical feedback associated with the changes in  $A$  as described in Bellon et al. (2003). Nevertheless, the variations of  $\Phi$  are fairly semestrial, with minima of similar amplitude in spring and fall, and maxima in summer and winter, while the boreal-fall maximum of  $A$  is significantly smaller than its maximum during boreal spring. Although changes in  $A$  can modulate  $\Phi$ , mechanisms other than the radiative control at play in two-column models account for the seasonal cycle of the tropical large-scale circulation. One of these mechanisms

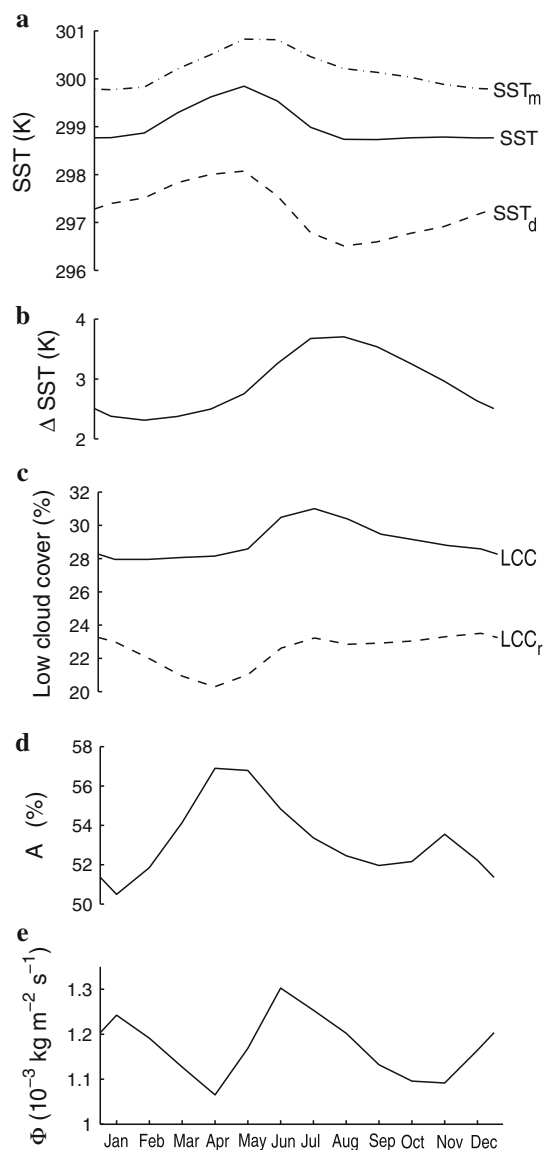


**Fig. 2** Seasonal cycles of (a) the tropical SST (solid line), dry-region SST ( $SST_d$  (dashed), and moist-regions  $SST_m$  (dash-dotted), (b) SST difference  $\Delta SST$  between moist and dry regions, (c) low-cloud cover in the dry tropical regions from ISCCP  $LCC$  (solid) and ERA40  $LCC_r$  (dashed), (d) relative size of the tropical moist regions  $A$ , and (e) normalized overturning circulation  $\Phi$

results from the dynamics of the Hadley circulation, the intensity of which depends on the location of convective heating: off-equatorial heating causes strong solstitial circulations, whereas near-equatorial heating causes weak equinoctial circulations (Lindzen and Hou 1988; Walker and Schneider 2005).

A more detailed analysis shows the complexity of the interaction between  $A$  and SST: as indicated by lag-correlations, variations of  $A$  tend to lag variations in the dry-region SST by about a month and to lead variations in the moist-region SST by one month. This suggests that the

winter warming of the dry regions participates to the growth of  $A$ : as  $SST_d$  increases, deep convection develops over a fraction of the dry regions, moistening the overlying column and increasing  $A$ .  $SST_m$  responds with a one-month lag because the release of latent heating and cloud radiative forcing associated to deep convection warms the troposphere rather than the surface. The energy is then redistributed to the surface by clear sky radiation and turbulent surface fluxes, through the restratification of the atmospheric column and the large-scale transport. The restratification is expected to happen on synoptic time-scales, but the large-scale transport involves longer time-scales, because it transits through the dry regions. Considering typical subsidence rates of about 50 hPa/day, a full cycle of the overturning circulation takes 40 days. The circulation therefore propagates an upper-tropospheric anomaly down to the dry surface and back to the moist regions in about a month. The one-month lag also corresponds to the adjustment timescale of the upper ocean to surface forcing. A thin, 10-meter-deep oceanic mixed layer adjusts by 1 K (typical of the SST seasonal cycle) to a surface forcing of  $10 \text{ Wm}^{-2}$  (typical of the surface-flux variations) in about 40 days. This combination of delays is a possible explanation for the lag between the seasonal cycle of  $A$  and that of  $SST_m$ . Beyond the influence of  $SST_d$ , the processes that control the seasonal cycle of  $A$  are unclear. Using a cloud-resolving model (CRM) over prescribed SSTs, Larson and Hartmann (2003) found a link between the SST gradients and the rain area at equilibrium. The SST difference between moist and dry regions  $\Delta SST = SST_m - SST_d$  (Fig. 2b) can be considered as a measure of SST gradients; we find no link between the seasonal cycles of  $\Delta SST$  and  $A$ . The winter and summer minima in  $A$  suggest a role of the monsoons in the seasonal cycle of  $A$ .

The relationship between the seasonal cycles of SST and  $LCC$  is more complex than the link between SST and  $A$ : from the two-column models, we expect an anticorrelation between SST and  $LCC$ , but the observed SST maximum seems to lead the observed  $LCC$  maximum by a few months (Fig. 2c). Nevertheless, there seems to be a local relationship between SST and  $LCC$  in the dry regions:  $SST_d$  exhibits a seasonal cycle opposite to that of  $LCC$ . The anticorrelation between  $SST_d$  and  $LCC$  peaks for a one-month lag (coefficient of  $-0.90$ ), similarly to the results of Norris and Leovy (1994) for interannual anomalies. This lag corresponds to the adjustment timescale of the upper ocean to surface forcing, as we pointed out in the previous paragraph. SST follows  $SST_d$  with a one-month lag, so that the anticorrelation between SST and  $LCC$  peaks for a two-month lag (coefficient of  $-0.74$ ).

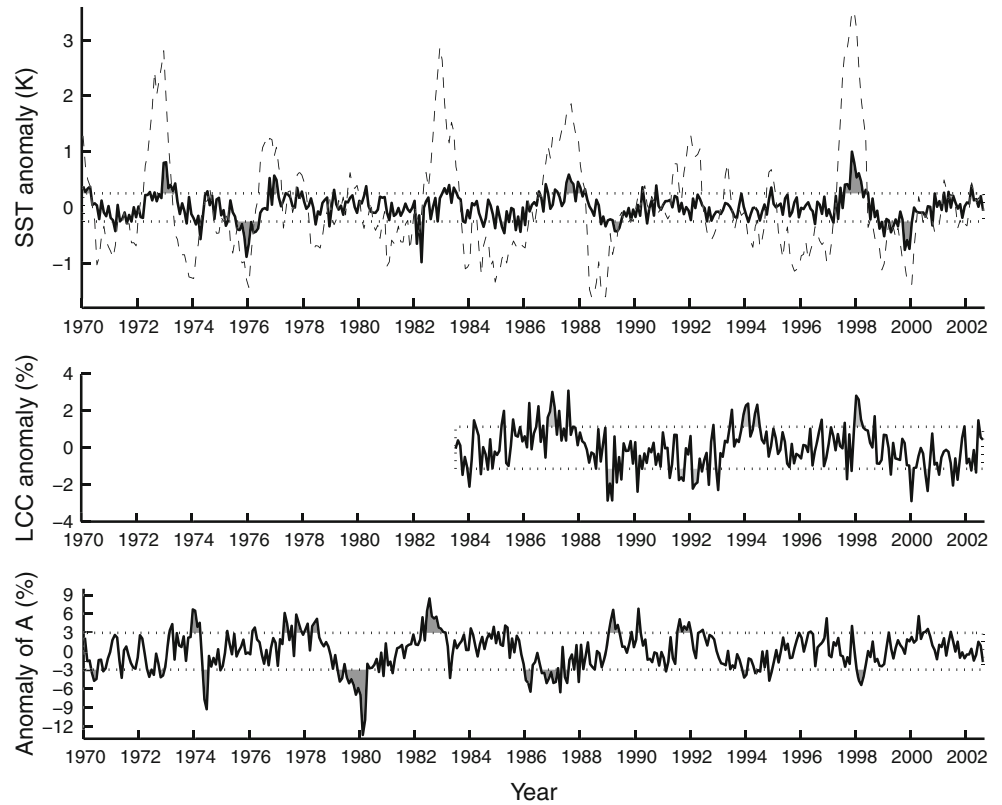
$LCC$  evolves similarly to the SST difference  $\Delta SST$  between moist and dry regions (Fig. 2b). The correlation peaks at zero lag (coefficient of 0.92).  $\Delta SST$  varies like the lower-tropospheric stability in the dry regions because tropical free-tropospheric temperature is fairly uniform on the horizontal and tied to the surface temperature in moist regions by deep convection (Sobel et al. 2002); therefore the observed link between  $\Delta SST$  and  $LCC$  is equivalent to the link between lower-tropospheric stability and  $LCC$  identified by Klein and Hartmann (1993). In their CRM experiments, Larson and Hartmann (2003) found the same relationship between SST gradients and low-cloud cover. Although an observed local relationship between vertical speed (subsidence) and low-cloud cover has been documented (Bony et al. 1997; Norris and Klein 2000), no such relationship appears in our synthetic analysis framework. In summary, the dry-region SST seems to respond locally to the low-cloud radiative forcing that is in turn controlled by the SST difference between convective and dry regions. The moist-region SST (Fig. 2a) adjusts slowly (on time-scales typical of the overturning circulation and upper-ocean adjustment) to the dry-region SST variations forced by  $LCC$ , mostly through the response of surface fluxes to the atmospheric changes.

### 3.2 Interannual variability

The interannual variability of the tropical SST,  $LCC$  and  $A$  are computed by subtracting the mean annual cycle from the time series, detrending (by removing the linear trend between the initial and final five-year averages) and filtering out decadal and multidecadal signals (removing the harmonics with periods longer than ten years using a simple Fourier transform). While this detrending and filtering does not influence our results significantly, it does improve the clarity of our figures. Figure 3 shows the resulting interannual anomalies. The filtered NINO3 index (SST anomaly in the eastern equatorial Pacific, averaged over the region  $5^\circ\text{N}$ – $5^\circ\text{S}$ ,  $150^\circ\text{W}$ – $90^\circ\text{W}$ ) is also shown in the upper panel of Fig. 3. The interannual variability of reanalyzed low-cloud cover  $LCC_r$  is well correlated with that of  $LCC$ , with larger anomalies (not shown). The reanalyzed low-cloud fields have previously been shown to exhibit a realistic interannual variability (Jakob 1999). The statistical analyses presented below yield the same qualitative results using  $LCC$  or  $LCC_r$ .

The interannual variability of the tropical SST is clearly dominated by the El Niño Southern Oscillation (ENSO). The correlation between the SST interannual anomalies and the NINO3 index is 0.61 and significant at the 99% level (and even at a much higher level). There is no

**Fig. 3** Interannual variability of the tropical SST, low-cloud cover in the dry tropical regions *LCC*, and relative size of the tropical moist regions *A*. Interannual standard deviations are shown by dotted lines and the NINO3 index is shown as a dashed line in the SST plot



obvious relationship between the interannual variability of SST and the interannual variations of *LCC* or *A*, except maybe for a tendency for *LCC* maxima and minima of *A* to happen during warm El Niño events. There is a actually significant correlation of 0.14 (respectively, a significant anticorrelation of  $-0.26$ ) between the SST anomalies and anomalies of *LCC* (respectively *A*). Correlations between the anomalies of *LCC* or *A* and the NINO3 index are significant as well (0.26 and  $-0.26$ ). This suggests that the fraction of interannual variability in *A* and *LCC* that is related to SST variability is driven by the ENSO. The signs of the correlations are opposite to the signs that would be expected if *LCC* and *A* were driving the interannual variability of SST according to the mechanisms identified in two-column models. This suggests that the ENSO drives the SST variability at interannual timescales, as well as variations of *A* and *LCC* that constitute negative feedbacks on the SST variability.

We can investigate whether the interannual variability in *A* and *LCC* that is not associated to the ENSO can account for some second-order SST variability independently from the first-order ENSO signal. In order to do so, we perform a linear regression of the SST variability on the NINO3 index and the anomalies of *A* or *LCC* for the available period (July 1983–August 2002):

$$SST' = \alpha_1 NINO3' + \alpha_2 X' + \epsilon, \quad (3)$$

where the prime denotes the interannual anomaly,  $X = A$  or *LCC*,  $\alpha_i (i = 1, 2)$  are regression coefficients and  $\epsilon$  is the residual.

To test the significance of the coefficients  $\alpha_i$  within this two-predictor model, we perform additional statistical tests to discriminate between the following hypotheses:

$$H_0 : \alpha_i = 0 \text{ (}\alpha_j \text{ being estimated);}$$

$$H_1 : \alpha_i \neq 0 \text{ (}\alpha_j \text{ being estimated);}$$

with  $(i, j) = (1, 2)$  or  $(2, 1)$ .

$\alpha_1$  is significant for both  $X = A$  and  $X = LCC$  (the  $p$  value of the corresponding statistical test is inferior to  $10^{-4}$ ) and the estimated coefficient is  $\alpha_1 = 0.17$  in both cases.

Table 1 shows the estimated coefficients  $\alpha_2$  and the  $p$  values associated to the statistical tests on  $\alpha_2$  for *A* and *LCC*. These coefficients are small: for a large change in *A* or *LCC* such as an additional 10% of cloud cover or moist fraction of the tropics, the associated change in SST

**Table 1** Regression coefficients  $\alpha_2$  for *A* and *LCC* from the regression of SST interannual anomalies on the NINO3 index and *A* or *LCC*, and  $p$  values of the corresponding statistical tests

$X$	$\alpha_2$	$p$ value
<i>A</i>	$-6.8 \cdot 10^{-3}$	0.14
<i>LCC</i> <sub>s</sub>	$-8.7 \cdot 10^{-3}$	0.42

would be less than 0.1 K. Moreover, in both cases, the null hypothesis cannot be rejected at the 95% confidence level (i.e., the  $p$  values are superior to 0.05). This shows that the interannual variations of  $A$  and  $LCC$  are not related to the interannual variability of SST independently of the ENSO.

These results show that the interannual variability of the tropical SST is mostly driven by internal dynamics of the tropical climate that are not represented in Pierrehumbert-like two-column models. El Niño Southern Oscillation is the main example of such internal dynamics of the tropical climate because of the large amplitude of its SST signal and because it is a coupled ocean-atmosphere mode of variability whose fundamental mechanisms involve ocean dynamics and ocean-atmosphere momentum transfer (Neelin et al. 1998) that are absent of Pierrehumbert-like models. The ENSO-related interannual variations of  $A$  and  $LCC$  constitute significant, negative feedbacks on SST variations: El Niño events are associated with a decrease in the relative area of moist regions and an increase in low-level cloudiness in the dry regions, potentially limiting the warming, but undoubtedly not driving it.

These relationships between the ENSO and  $A$  or  $LCC$  contrast with previous studies. El Niño events are often pictured as an expansion of the Western Pacific warm pool into the Central Equatorial Pacific associated with an expansion of the overlying deep-convective region. We would therefore expect an increase in  $A$  during warm phases of the ENSO. Our two-column analysis delivers a different picture: moist regions tend to shrink during warm events. Figure 4 shows the approximate boundary between moist and dry regions during El Niño and La Niña events. Indeed, the moist regions extend further in the equatorial Pacific during El Niño, but they extend further in the subtropics over the Western Pacific during La Niña, yielding a larger ratio of moist regions during cold events than during warm events. Figure 4 shows that the El Niño pattern is more zonally symmetric than the La Niña pattern. This illustrates the opposite modulations of the Hadley cell and the Walker circulation by the ENSO (Oort and Yienger 1996).

Previous studies have also associated warm ENSO events to a decrease of low-cloud cover in the Eastern Pacific basin, both over the equator and in the subtropical

stratocumulus decks (Bajuk and Leovy 1998; Zhu et al. 2007). Our two-column analysis shows that over all, the low-cloud cover increases in the dry regions during warm events. Figure 5 shows the contribution of each gridpoint to the regression coefficient of  $LCC$  on the NINO3 index. This regression coefficient equals the spatial integral of the plotted contribution, and it is positive. The Eastern Pacific contributes negatively to this coefficient, particularly over the equatorial cold tongue and at the poleward edges of the subtropical stratocumulus decks. But this signal is exceeded by the positive contribution of the subtropical Western and Central Pacific, where small cumuli are found. Part of these positive pattern, as well as the negative pattern over the equatorial cold tongue, results from the changes in the geographical distribution of moist and dry regions (see Fig. 4). Regions that are excluded from the dry regions during El Niño (respectively La Niña) events contribute negatively (respectively positively) to the regression coefficient of  $LCC$  on the NINO3 index.

We further investigate the relationship between  $LCC$  and the large-scale environment. Our analysis does not find any correlation between the interannual variability of  $LCC$  and the SST in dry regions: the regional lag-correlations found by Norris and Leovy (1994) do not appear in our synthetic two-column framework. We find no relationship between  $LCC$  and subsidence in the dry regions either. But we find a significant correlation of 0.37 between the interannual anomalies of  $LCC$  and  $\Delta SST$  that suggests a control of the lower-tropospheric stability on the low-cloud cover (Klein and Hartmann 1993) on interannual scales. This is similar to the relationship found for seasonal cycles, and consistent with previous model results (Larson and Hartmann 2003). Note that  $\Delta SST$  and the NINO3 index are uncorrelated, so that the control of  $LCC$  by  $\Delta SST$  is independent from the ENSO.

#### 4 Summary and discussion

We have proposed a method based on physical criteria to interpret the actual tropical climate in a two-column framework. Following this method, the tropics are defined as the longitudinal belt where the Hadley circulation is

**Fig. 4** Boundary between moist and dry regions during El Niño (solid) and La Niña (dotted) events. The boundary is defined as the 50% isoline of the probability of an atmospheric column to be moist or dry during El Niño or La Niña events

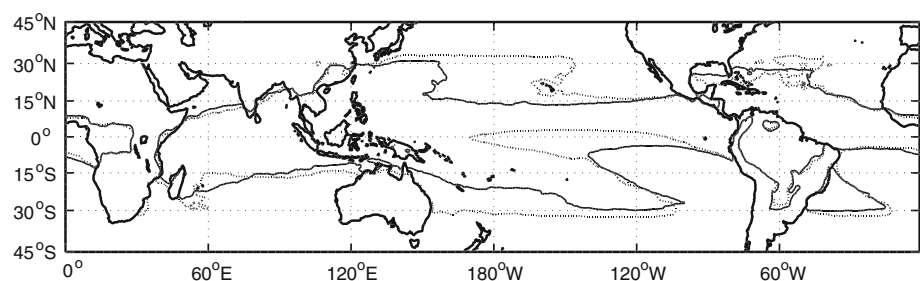
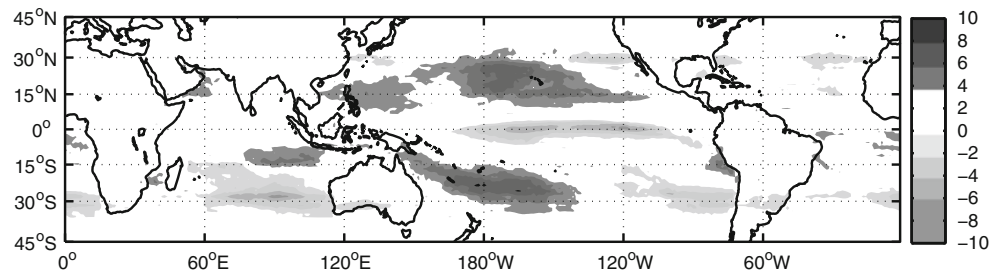


**Fig. 5** Contribution of each gridpoint to the regression coefficient of *LCC* on the NINO3 index (in  $10^{-14} \%K^{-1} m^{-2}$ ). The regression coefficient is the spatial integral of this contribution



enclosed, and a humidity variable closely related to precipitation is used to distinguish between moist and dry regions. Using this method, the natural variability of the tropical climate can be interpreted in terms of the main variables and parameters of the two-column models. We focus on the relationship between the tropical SST and the main parameters that have been identified as important in these models. The results are contrasted.

The seasonal cycle of the tropical SST is dominated by a strong boreal spring (pre-monsoon) maximum. It is strongly correlated with the seasonal cycle of the relative area of the moist regions *A*; this results from a non-instantaneous interaction between the dry and moist regions through the overturning circulation and upper-ocean adjustment. The SST in the dry regions seems to respond to the *LCC* forcing with a one-month lag, and the tropic-wide SST adjusts with a two-month lag. *LCC* appears to be controlled by the SST difference between moist and dry regions; this suggests a control of *LCC* by the lower-tropospheric stability in the dry regions. These results show that the contribution of *A* and *LCC* to the seasonal cycle of the tropical SST can be understood in our two-column framework, but in a more complex fashion than the quasi-equilibrium sensitivity depicted by simple two-column models.

On the other hand, the interannual variability of the tropical SST is dominated by the El Niño Southern Oscillation signal and does not appear to be related to the variability of *A* or *LCC* independently of the ENSO. Changes in *A* and *LCC* associated to the ENSO constitute small negative feedbacks to the ENSO-related SST variability.

One possible interpretation of these results is that the El Niño Southern Oscillation is an internal mode of the tropical ocean-atmosphere coupled system involving processes that are not represented in the idealized two-column models, with additional feedbacks and imbalances that render the two-column feedbacks ineffective. On the other hand, the seasonal cycle of the tropical climate can be considered as a response to a perturbation of the solar forcing, and two-column models are thought to be appropriate to assess this response. But, even in the case of the seasonal cycle, the link between SST and *A* or *LCC* is not instantaneous.

Our results clearly show some limits of the simple two-column models. Still, because such models are tailored to assess the response to radiative perturbations such as the solar annual cycle and CO<sub>2</sub> doubling, they might be relevant in interpreting some features of climate change in the tropics. In particular, recent observations show both a drying trend at the margins of some TCZs (Neelin et al. 2006) and a widening of the Hadley circulation (Seidel et al. 2008). In the two-column framework, these trends can be interpreted as a decrease in *A<sub>m</sub>* and an increase in *A<sub>r</sub>*. Both result in a decrease of *A* and should constitute a negative feedback on the tropical warming, at the expense of water resources in the margins of the dry subtropics. The mechanisms involved in these potential feedbacks are still unclear.

**Acknowledgements** The author would like to thank J.-L. Redelsperger for comments that inspired this work and D. Bellon for editing the manuscript.

## References

- Bajuk LJ, Leovy CB (1998) Seasonal and interannual variations in stratiform and convective clouds over the tropical Pacific and Indian oceans from ship observations. *J Clim* 11(11):2922–2941
- Bellon G, Le Treut H, Ghil M (2003) Large-scale and evaporation-wind feedbacks in a box model of the tropical climate. *Geophys Res Lett* 30:2145. doi:10.1029/2003GL017895
- Bony S, Dufresne JL (2005) Marine boundary layer clouds at the heart of tropical cloud feedback uncertainties in climate model. *Geophys Res Lett* 32:L20806. doi:10.1029/2005GL023851
- Bony S, Lau KM, Sud YC (1997) Sea surface temperature and large-scale circulation influences on tropical greenhouse effect and cloud radiative forcing. *J Clim* 10:2055–2077
- Bretherton CS, Peters ME, Back LE (2004) Relationships between water vapor path and precipitation over the tropical oceans. *J Clim* 17:1517–1528
- Clement AC, Burgman R, Norris JR (2009) Observational and model evidence for positive low-level cloud feedback. *Science* 325(5939):460–464. doi:10.1126/science.1171255
- Cronin M, Bond N, Fairall C, Weller R (2006) Surface cloud forcing in the East Pacific stratus deck/cold tongue/ITCZ complex. *J Clim* 19(3):392–409
- Dufresne JL, Bony S (2008) An assessment of the primary sources of spread of global warming estimates from coupled atmosphere-ocean models. *J Clim* 21(19):5135–5144
- Held IM, Hou AY (1980) Nonlinear axially symmetric circulations in a nearly inviscid atmosphere. *J Atmos Sci* 37:515–533



- Ide K, Le Treut H, Li ZX, Ghil M (2001) Atmospheric radiative equilibria. Part II: bimodal solutions for atmospheric optical properties. *Clim Dyn* 18:29–49
- Jakob C (1999) Cloud cover in the ECMWF reanalysis. *J Clim* 12(4):947–959
- Klein SA, Hartmann DL (1993) The seasonal cycle of low stratiform clouds. *J Climate* 6:1587–1606
- Larson K, Hartmann DL (2003) Interactions among cloud, water vapor, radiation, and large-scale circulation in the tropical climate. Part II: sensitivity to spatial gradients of sea surface temperature. *J Clim* 16(10):1441–1455
- Larson K, Hartmann DL, Klein SA (1999) The role of clouds, water vapor, circulation, and boundary layer structure in the sensitivity of the tropical climate. *J Clim* 12:2359–2374
- Lindzen RS, Hou AY (1988) Hadley circulations for zonally averaged heating centered off the equator. *J Atmos Sci* 45:2416–2427
- Miller RL (1997) Tropical thermostats and low cloud cover. *J Clim* 10:409–440
- Neelin JD, Battisti DS, Hirst AC, Jin FF, Wakata Y, Yamagata T, Zebiak S (1998) Enso theory. *J Geophys Res Atmos* 103 (C7):14261–14290
- Neelin JD, Munnich M, Su H, Meyerson JE, Holloway CE (2006) Tropical drying trends in global warming models and observations. *Proc Natl Acad Sci* 103:6110–6115
- Nilsson J, Emanuel KA (1999) Equilibrium atmospheres of a two-column radiative-convective model. *Q J R Meteorol Soc* 125:2239–2264
- Norris JR, Klein SA (2000) Low cloud type over the ocean from surface observations. Part III: relationship to vertical motion and the regional surface synoptic environment. *J Clim* 13:245–256
- Norris JR, Leovy CB (1994) Interannual variability in stratiform cloudiness and sea surface temperature. *J Clim* 7(12):1915–1925
- Oort AH, Rasmusson EM (1970) On the annual variation of the monthly mean meridional circulation. *Mon Weather Rev* 98:423–442
- Oort AH, Yienger JJ (1996) Observed interannual variability in the Hadley circulation and its connection to ENSO. *J Clim* 19(11):2751–2767
- Pierrehumbert RT (1995) Thermostats, radiator fins, and the local runaway greenhouse. *J Atmos Sci* 52:1784–1806
- Raymond DJ, Zeng X (2000) Instability and large-scale circulations in a two-column model of the tropical troposphere. *Q J R Meteorol Soc* 126 (570):3117–3135
- Rennó NO (1994) Multiple equilibria in radiative-convective atmospheres. *Tellus A* 49:423–438
- Schiffer RA, Rossow WB (1983) The international satellite cloud climatology project (ISCCP): The first project of the world climate research programme. *Bull Am Meteorol Soc* 64:779–784
- Seidel D, Fu Q, Randel W, Reichler T (2008) Widening of the tropical belt in a changing climate. *Nat Geosci* 1:21–24
- Simmons AJ, Gibson JK (2000) The ERA-40 project plan. ERA-40 project report series No. 1. European Centre for Medium-range Weather Forecast, Reading
- Sobel AH, Held IM, Bretherton CS (2002) The ENSO signal in tropical tropospheric temperature. *J Clim* 15:2702–2706
- Sobel AH, Bellon G, Bacmeister JT (2007) Multiple equilibria in a single-column model of the tropical atmosphere. *Geophys Res Lett* 34:L22804. doi:[10.1029/2007GL031320](https://doi.org/10.1029/2007GL031320)
- Stevens B, Beljaars A, Bordoni S, Holloway C, Khler M, Krueger S, Savic-Jovicic V, Zhang Y (2007) On the structure of the lower troposphere in the summertime stratocumulus regime of the northeast Pacific. *Mon Weather Rev* 135:985–1005
- Walker C, Schneider T (2005) Response of idealized Hadley circulations to seasonally varying heating. *Geophys Res Lett* 32:L06813
- Weare BC (2000) Near-global observations of low clouds. *J Clim* 13(7):1255–1268
- Zhang C, Mapes BE, Soden BJ (2003) Bimodality in tropical water vapour. *Q J R Meteorol Soc* 129:2849–2866
- Zhu P, Hack JJ, Kiehl JT, Bretherton CS (2007) Climate sensitivity of tropical and subtropical marine low cloud amount to ENSO and global warming due to doubled CO<sub>2</sub>. *J Geophys Res Atmos* 112:D17108. doi:[10.1029/2006JD008174](https://doi.org/10.1029/2006JD008174)